

A Novel Circularly Polarized Annular Slotted Multiband Rectenna for Low Power Sensor Applications

Neeru Kashyap¹, Geetanjali¹, and Dhawan Singh^{2, *}

Abstract—To overcome electronic device dependence on energy storage medium, current research proposes a novel multiband circularly polarized (CP), microstrip patch antenna with a voltage multiplier rectifier circuit for wireless energy harvesting. The proposed antenna is designed with a dimension of $50\text{ mm} \times 50\text{ mm} \times 0.16\text{ mm}$ ($0.80\lambda \times 0.80\lambda \times 0.028\lambda$). Its annular slot and slits on a circular patch along with a defective ground plane result in a miniaturized, circularly polarized, and multiband response with resonance peaks at 6.3 GHz, 7.4 GHz, and 9.1 GHz, respectively. The voltage multiplier rectifier circuit is designed, optimized, and integrated with the antenna for RF signals to DC power conversion in order to energize low-power sensors-based application modules. The simulated multiband antenna resonates at three frequencies of 6.3 GHz, 7.4 GHz, and 9.1 GHz with obtained -10 dB impedance bandwidths of 282 MHz (6.276 GHz–6.549 GHz), 178 MHz (7.348 GHz–7.526 GHz), and 81 MHz (9.136 GHz–9.217 GHz), gain of 6.3 dBi, 10.28 dBi, and 7.9 dBi, and axial ratio bandwidth of (6.297 GHz–6.302 GHz), (7.783 GHz–7.411 GHz), and (9.256 GHz–9.473 GHz), respectively. The prototype is fabricated, and its resonance peaks are observed at 6.2 GHz, 7.8 GHz, and 9.3 GHz, with impedance bandwidth of 195 MHz, 206 MHz, and 230 MHz and gain of 6.3 dBi, 9.6 dBi, and 7.4 dBi, respectively. The rectifier circuit is analyzed over the power range -20 dBm to 20 dBm and exhibits an increase in the DC output power significantly with a maximum measured efficiency of 53.34% at a frequency of 7.4 GHz with an associated load resistance of $1\text{ k}\Omega$.

1. INTRODUCTION

Today, wireless sensors are employed in a wide range of applications such as civilian and industrial applications, smart agriculture, smart buildings, smart cities, smart health care system, smart education, and other services [1–3]. Smart sensors-based modules are widely deployed in several gadgets, systems, and devices, which require a steady energy source to power them up. One of the effective solutions is to use an AC power supply from the grid to power these modules. However, the problem persists when wireless modules are located remotely with no available source of electricity. Another solution is to use a battery as a source of electricity; however, it also has several flaws including time-to-time charging, limited power capacity, short lifespan, high cost, and others.

Energy can be harvested in nature from various external sources such as solar, wind, thermal, salinity, vibration, kinetic energy, and radio frequency (RF) energy [4, 5]. Fig. 1 depicts the various energy harvesting sources that may be naturally found. Out of these sources, RF energy harvesting is an energy conversion technique used to convert electromagnetic energy into a usable energy source [6]. This will be utilized to power electronic devices from the distance and helps in extending battery life. It is one of the most suitable and feasible methods as it captures energy directly from various RF sources including wireless base stations, mobile phones, Wi-Fi, satellite devices, wireless networks,

Received 26 December 2022, Accepted 10 March 2023, Scheduled 21 March 2023

* Corresponding author: Dhawan Singh (dhawan_deor@yahoo.co.in).

¹ Chitkara University Institute of Engineering and Technology, Chitkara University, Punjab, India. ² University Centre for Research & Development, Chandigarh University, Mohali, Punjab 140103, India.

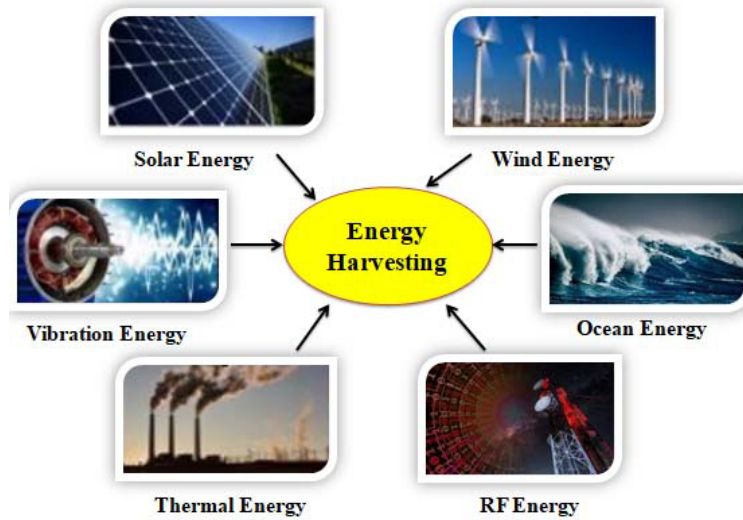


Figure 1. Energy harvesting sources.

FM/AM radio station and TV towers, wireless internet, dedicated transmitters, and other sources [7–9]. The critical feature of RF energy harvesting (RFEH) is that it is not time-dependent, and the energy collected from the surrounding environment can be converted to acceptable DC power at any time of day or night, in any season, under any weather condition, and both indoors and outdoors [10, 11].

Researchers have been currently working on RFEH systems, which harvest RF power and convert it to DC power to energize the low-power sensors used in smart devices and systems [12, 13]. Fig. 2 shows the block diagram of the RFEH system which consists of a receiving antenna, impedance matching network, rectifier circuit, and charging circuit. A compact planar receiving antenna, particularly for portable handheld devices, is in high demand for efficient energy harvesting. Furthermore, it is required to have a very compact geometry with multiband, high-gain, efficient radiation-efficiency, and circular polarization [14–16]. Single-band or dual-band antennas have been used in literature for RFEH; however, they have limitations as not efficient to capture RF energy from different frequency bands. In addition to this, circularly polarized antennas are preferred as it allows polarization in all directions without worrying about the vertical/horizontal alignment [17]. However, RFEH supported receiving antenna has many challenges to overcome such as the size, geometry, planar structure, multiband polarization, frequency, bandwidth, sensitivity, and efficient radiation [18, 19].

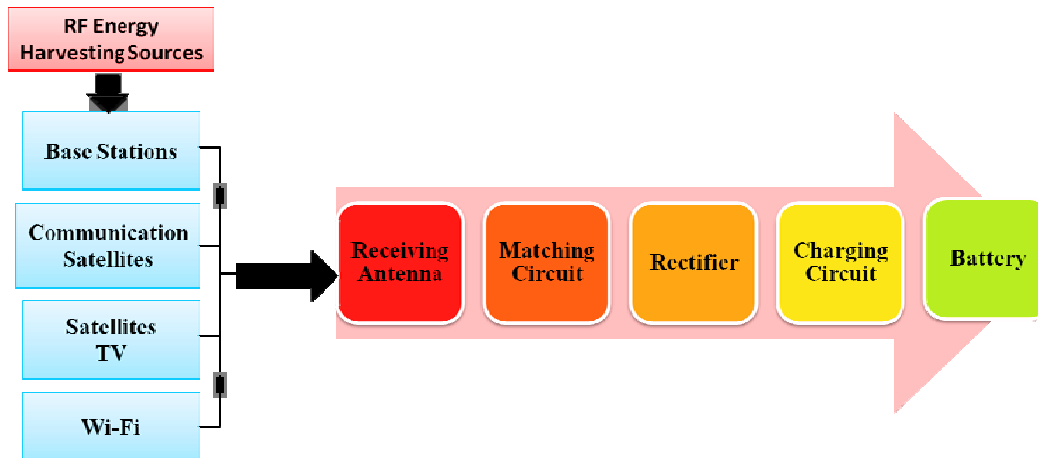


Figure 2. Block diagram of rectenna.

Incoming EM waves from the transmitting source should be efficiently captured and transferred to the rectifier section for final DC conversion. RFEH technology has been recently introduced to the research field, with a few researchers working on the efficiency and design perspective of RF energy harvesting systems, such as multiband with a circular polarization rectenna (antenna + rectifier), reported in the literature [20–22].

A recent method employs multiband antennas to increase the amount of energy captured by multiband energy harvesting [23–25]. However, in order to achieve a high conversion efficiency at a low input power density, this research work requires a large load. Furthermore, circularly polarized (CP) rectennas have been employed to improve conversion efficiency due to their flexibility in electromagnetic transmission [26–28]. Taking these factors into account, the current research work proposes a multiband antenna with excellent response at 900 MHz, 1.8 GHz, 2.5 GHz, and 5.2 GHz, respectively. With the use of a wideband energy harvester, a high output voltage has been promised in order to collect more RF signals from various frequency bands. However, the limitations could include the decreased conversion efficiency caused by frequency-dependent change, which makes it challenging to maintain the impedance match across a broad frequency range. Henceforth, energy harvesting from many narrow frequency bands is preferable compared to a single wide one to solve this problem [29, 30].

Tran et al. proposed a dual-band, circularly polarized antenna by using feeding methods between the frequency ranges of 5 GHz to 5.9 GHz. The gain obtained by the antenna is 6.6 dBi; however, it lacks a multiband spectrum response [31]. Ghosh proposed a circularly polarized microstrip antenna. Square ring slotting technique is used for GSM 900 band for RFEH rectenna applications. The highest gain of 17 dB was achieved for a 100 m distance, and good gain is achieved at a single frequency. This research work again misses multiband capabilities [32]. Garlapati et al. proposed a circle-shaped patched multiband antenna with circular polarization and employed the aid of a substrate integrated waveguide structure. This antenna is created using cross-shaped square slots with vias, swastika, and coaxial single-feeding techniques. The antenna achieved gains of 10.28 dB, 3.54 dB, 8.73 dB, and 3.72 dB at various frequencies such as 3.16 GHz, 6.35 GHz, 8.4 GHz, and 9.85 GHz. However, rectifier circuit for the designed antenna was not available in the research work [33]. Mouapi et al. proposed an antenna with a rectifier circuit for 1800 MHz with the size of the rectifier being 45×45 mm and achieved an efficiency of 61% [34]. Ali et al. proposed an antenna with a rectifier circuit with a rectifier size of 40×40 mm at 2.45 GHz frequency and achieved an efficiency of 86% [35]. Elsheakh et al. proposed a rectenna operating at four frequency bands 900 MHz, 1.8 GHz, 2.5 GHz, and 5.2 GHz and achieved a maximum power conversion efficiency of 56.4% at 1.8 GHz [36]. Singh et al. designed a multiband antenna with a rectifier of a size 60×60 mm but achieved circular polarization only for dual-band antenna [37].

In this literature review, many have achieved dual-band or multiband responses for RF energy harvesting, whereas only a few have achieved the circular polarization response, and it is always challenging for multiband antennas. The current study focuses on the analysis, design, and fabrication of an RFEH antenna to achieve a multiband band response with circular polarization using several design techniques such as slits, slotting, and defected ground structure (DGS). The proposed model is appropriate for RF energy harvesting in low-power sensors, among other applications.

The paper is organized into different sections as follows. The specifications for the antenna design, geometry, optimization, and its various characteristic using step-by-step parametric variation are provided in Section 2. Comparison of simulated and measured results with discussions such as the antenna reflection coefficient, surface current distribution, axial ratio, gain, radiation pattern at E -plane and H -plane, and voltage standing wave ratio (VSWR) characteristics at the resonant frequencies of the proposed antenna is presented in Section 3. The design of the rectifier circuit for a multiband circularly polarized antenna is presented in Section 4. All measurement results of the fabricated antenna and fabricated rectifier circuit are discussed in Section 5. Finally, the conclusion is drawn, and future recommendations are given in Section 5.

2. DESIGN STRUCTURE AND OPTIMIZATION OF ANTENNA SYSTEM

In this research paper, a circularly polarized annular slot microstrip antenna with slits on the patch and ground plane is designed for harnessing RF energy from multiple bands and further integrated with

a rectifier circuit with a voltage multiplier for efficient conversion of RF energy to DC output power which is capable of driving low power sensors deployed in wireless communications.

2.1. Design Consideration of Antenna

The design layout of the proposed antenna structure is depicted in Fig. 3. The designed antenna has an overall dimension of $50\text{ mm} \times 50\text{ mm}$. FR-4 is used as a substrate with $\epsilon_r = 4.4$, and a standard thickness of 1.6 mm is considered. For achieving the multiband operation and circular polarization, the proposed antenna is designed by modifying a normal circular patch with an annular slot, slits, and DGS, respectively. The optimized antenna parameters and their dimensions are shown in Table 1. This optimized antenna structure achieves better radiation performance and high gain along with the antenna's miniaturization. The front view is shown in Fig. 3(a), whereas the back view is presented in Fig. 3(b).

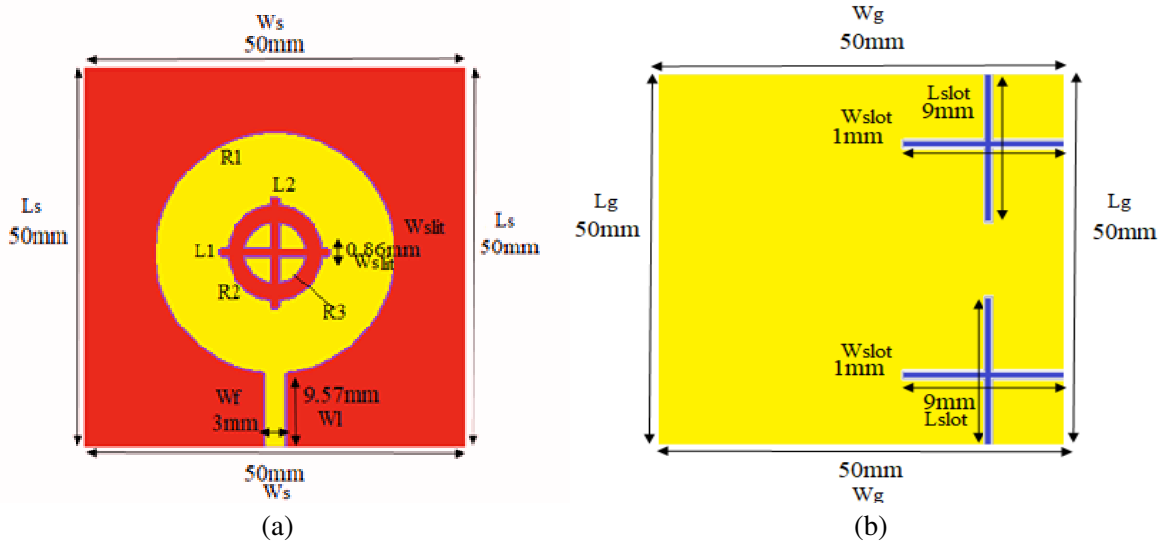


Figure 3. (a) Front view and (b) back view of the proposed antenna.

Table 1. Dimension of proposed microstrip patch antenna.

Parameter	Description	Value (mm)
$R1$	Radius of circle patch	15.5
$R2$	Outer radius of ring slot	6
$R3$	Inner radius of ring slot	4
W_{slit}	Width of slits	0.86
W_s	Width of substrate	50
L_s	Length of substrate	50
W_g	Width of ground	50
L_g	Length of ground	50
L_f	Length of feedline	9.57
$L1$	Length of slits	14
$L2$	Length of slits	14
W_f	width of feedline	3
L_{slot}	Length of DGS slot	9
W_{slot}	Width of DGS slot	1

2.2. Step Wise Antenna Evolution

The proposed patch antenna is optimized in four steps, as illustrated in Fig. 4. To begin with, a circular radiating patch is designed and forms a defected ground structure in the ground plane. Circular polarization and optimization of the antenna are obtained by DGS in the ground, an annular slot and slits in the radiating patch. Fig. 5 shows a comparison of the reflection coefficient obtained during the antenna evolution from Antenna 1 to Antenna 4. The number of frequency bands achieved for the antenna and the corresponding reflection coefficient is significantly improved during the antenna evolution as shown in Fig. 5. In Antenna 1, the proposed antenna operates in dual resonant bands at 5.3 GHz and 7.4 GHz with $S_{11} < -22$ dB and < -34 dB, respectively. Antenna 1 is modified by adding two slits at the difference of 90° in a circular radiating patch to form Antenna 2 which resonates over a single frequency band at 5.4 GHz with $S_{11} < -15$ dB. To cause multiple resonances, an annular type slot is added to the radiating patch to form Antenna 3 which radiates at frequency bands 6.3 GHz and 9.0 GHz with $S_{11} < -14$ dB and -19 dB, respectively. In Antenna 4, by adding a defected ground structure in the ground plane, the suggested antenna is successfully operated at the desired three frequency bands.

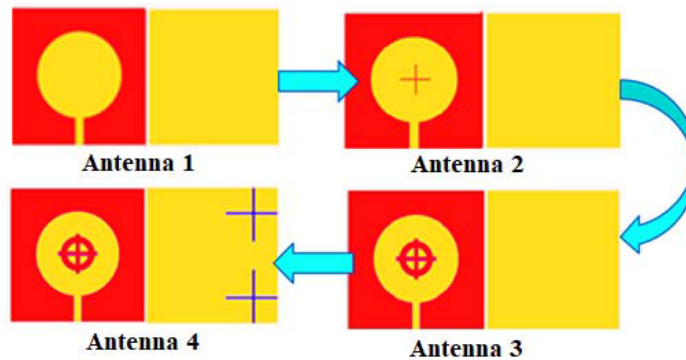


Figure 4. Proposed antenna designing steps wise.

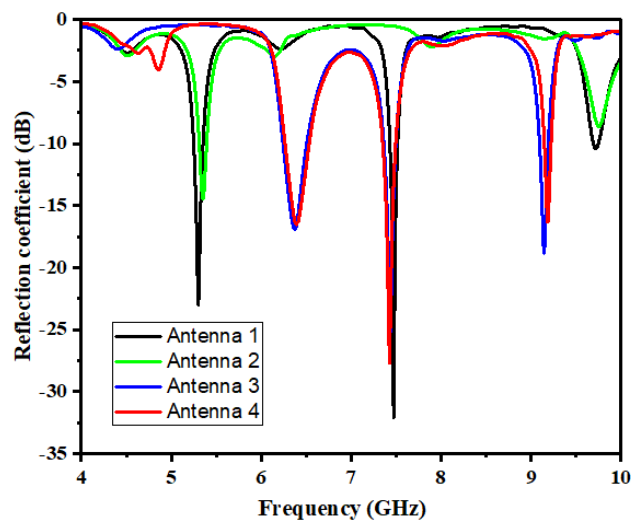






Figure 5. Step-wise reflection coefficient of proposed antenna.

The designed antenna is perfectly matched with 50Ω impedance and operates at three frequencies with reflection coefficients of -16.54 dB, -28.36 dB, and -15.87 dB as depicted in Fig. 5. Moreover, the circular polarization is also achieved in the proposed multiband microstrip antenna. Finally, the circularly polarized multiband antenna is resonant at three frequencies which are 6.3 GHz, 7.4 GHz,

and 9.1 GHz with obtained -10 dB bandwidths of 282 MHz, 178 MHz, and 81 MHz, respectively. The antenna evolution and its simulation results are summarized in Table 2.

Table 2. Step-wise antenna evolution with parameters.

Antenna	Techniques	Antenna Image	Resonant Frequency	Reflection coefficient	Gain	Achieved Circular Polarization	Bandwidth
Antenna 1	Simple Circular Patch		5.3 GHz 7.4 GHz	-22.2 dB -34.2 dB	4.6 dBi 10.49 dBi	No	122 MHz 114 MHz
Antenna 2	Annular slot and slits on circular patch		5.4 GHz	-15.1 dB	4.0 dBi	No	282 MHz
Antenna 3	Annular slot and slits on circular patch without DGS		6.40 GHz 7.34 GHz 9.19 GHz	-15.90 dB -26.14 dB -11.15 dB	6.3 dBi 10.08 dBi 7.96 dBi	No Yes yes	253 MHz 195 MHz 071 MHz
Antenna 4 (Proposed Antenna)	Annular slot and slits on circular patch with DGS		6.37 GHz 7.42 GHz 9.19 GHz	-16.54 dB -28.36 dB -23.87 dB	6.3 dBi 10.28 dBi 7.91 dBi	Yes	282 MHz 178 MHz 81 MHz

3. MULTIBAND CIRCULARLY POLARIZED ANTENNA WITH RESULTS AND DISCUSSIONS

3.1. Reflection Coefficient

In Fig. 6, the reflection coefficient of the proposed antenna shows that the antenna resonates at frequencies of 6.3 GHz, 7.4 GHz, and 9.1 GHz with the appreciable values of reflection coefficients of -16.54 dB, -28.36 dB, and -15.87 dB and achieved bandwidths of 28 MHz, 178 MHz, and 81 MHz, respectively.

3.2. Surface Current Distribution and Phase Difference of Circular Polarization Proposed Antenna Mechanism

Figure 7 shows the surface current density of the proposed antenna in all three resonating frequency bands giving a better understanding of the behavior of the antenna by signifying the contribution in the far-field of the proposed antenna. The proposed antenna is excited by applying the appropriate power to the radiating patch through the feed line which causes the current flow in different regions of the patch and creates resonance at different frequencies. The periphery of the circle and the surface of the patch excluding the annular slot show the highest current density at a frequency 6.3 GHz. The current is distributed along the upper and lower halves of the circular patch at a frequency 7.4 GHz. Different modes of current are excited at 9.1 GHz, which can be seen to contribute to the radiation in the circular patch. The simulated current distributions with different phases at 0° and at 90° of the proposed

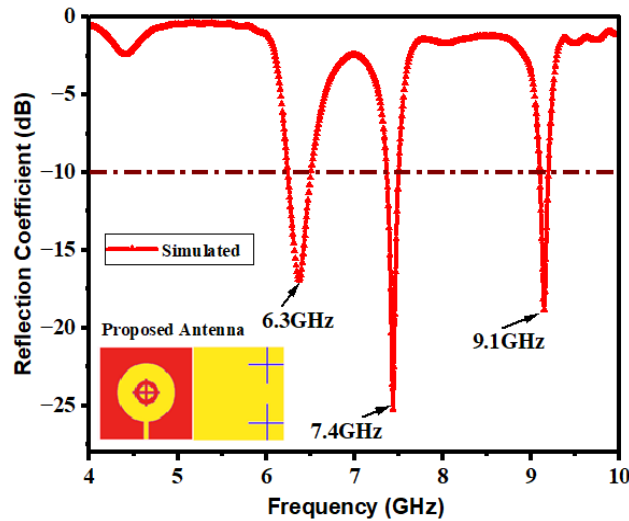


Figure 6. Reflection coefficient results of the proposed antenna.

structure are illustrated in Fig. 7 at resonant frequencies of 6.3 GHz, 7.4 GHz, and 9.1 GHz. Results are shown in Figs. 7(a), (c), (e) at 0° phase, and here the resonances are formed due to the current flow reaching the maximum magnitude in the $+x$ direction. In Figs. 7(b), (d), (f) at 90° , the current distributes in the $-x$ direction. Therefore, the observed resultant current distributes in anticlockwise direction, henceforth a left-hand circular polarization (LHCP) is achieved.

3.3. Gain Enhancement

Figure 8 depicts the simulated and measured gains of the proposed antenna at three different frequency bands. At 6.3 GHz, the simulated gain obtained is 6.3 dBi, and the measured gain obtained is 6.3 dBi. At 7.4 GHz, the simulated gain achieved is 10.28 dBi, and the measured gain is 9.6 dBi. At 9.1 GHz, simulated gain is 7.9 dBi, and the measured gain is 7.4 dBi. A good value of gain is achieved across all working frequency bands with a maximum gain of 10.28 dBi (simulated) and 9.6 dBi (measured) at 7.4 GHz frequency, respectively.

3.4. Axial Ratio and VSWR

The graph of circular polarization and VSWR for the proposed antenna is depicted in Figs. 9(a) and (b), respectively. Antenna is circularly polarized when the two orthogonal electric fields, the horizontal electric field (E_x) and vertical electric field (E_y), should have equal amplitudes and a phase difference (PD) of 90° all over the bands of relevance. At all three resonant frequencies, the amplitude of the axial ratio pattern is < 3 dB. We also achieved CP which can be seen in Fig. 9. Axial ratio graph depicts the corresponding calculated amplitude ratio (E_x/E_y) and phase difference of the two orthogonal electric field components. This helps us to clearly understand the performance of proposed antenna's CP excitation, which causes the antenna to be circularly polarized, enables the antenna to harvest energy from all directions effectively irrespective of its orientation, and is responsible for the overall better performance of the antenna. VSWR (Voltage Standing Wave Ratio) is shown in Fig. 9(b) which lies within 1 and 2 at the three different resonant frequencies of 6.3 GHz, 7.4 GHz, and 8.0 GHz, respectively.

3.5. Radiation Patterns of Circularly Polarized Multiband Antenna

The proposed antenna is tested in an RF anechoic chamber, as depicted in Figs. 10(a) and (b), and the radiation pattern is plotted in both the azimuth and the elevation planes.

The simulated and measured radiation polar plots in E -plane circularly polarized multiband antenna are depicted in Figs. 11(a), (b), and (c), and radiation polar plots in H -plane are depicted

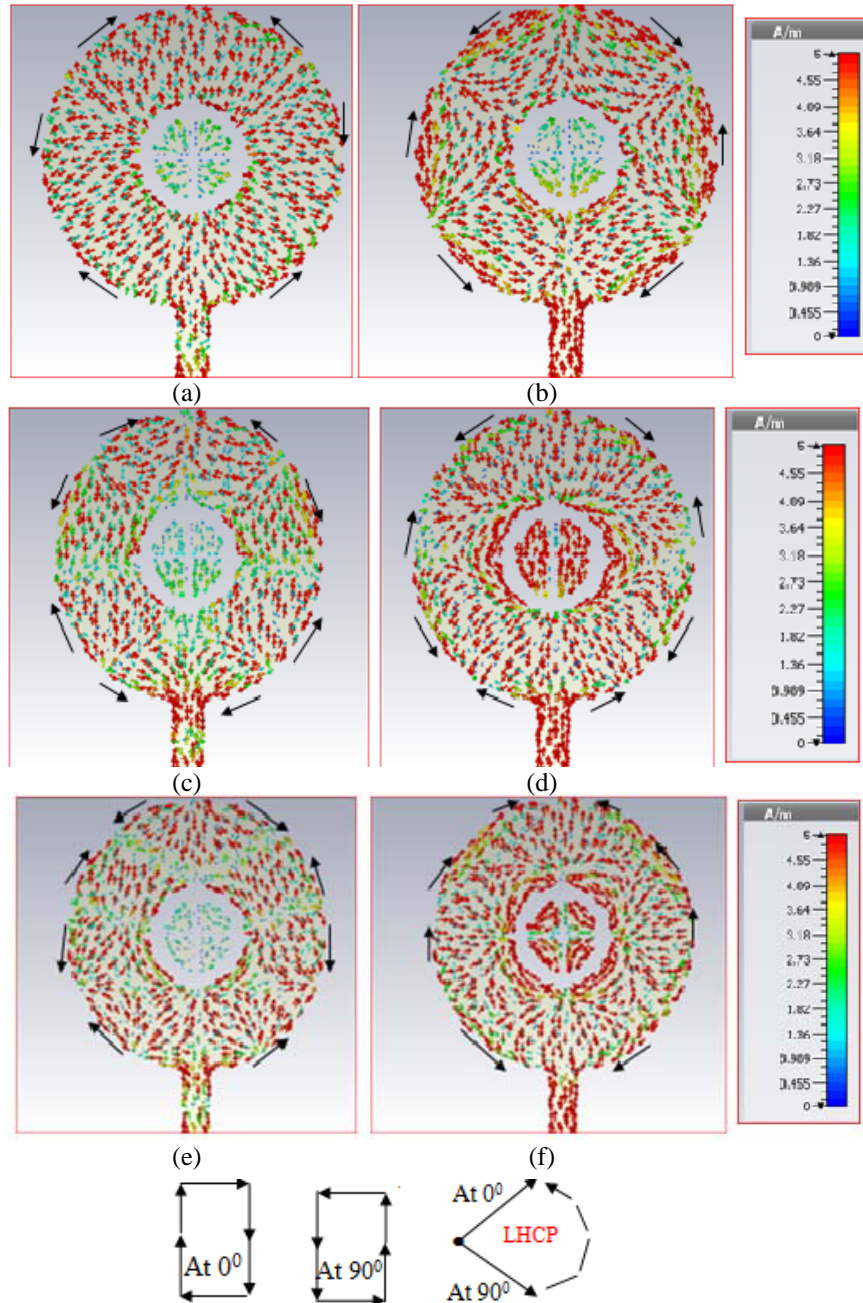


Figure 7. Simulated surface current distribution (A/m) (a), (c), (e) at 0° and (b), (d) and (f) at 90° resonant frequencies of 6.3 GHz, 7.4 GHz and 9.1 GHz.

in Figs. 11(d), (e), and (f), respectively. The simulation of the proposed antenna displays the radiation pattern is in LHCP pattern at the resonant frequencies of 6.3 GHz, 7.4 GHz, and 9.1 GHz. The radiation pattern shows an almost omnidirectional pattern in the E -plane (azimuthal plane), and somewhat directional lobes are seen in the H -plane elevation plane.

Finally, Table 3 shows a comparison of the proposed antenna with other high-gain dual and multiband circular polarization antennas studied in the literature. As can be seen, the proposed design has a unique structure with slits and slots for achieving high gain and circular polarization, which makes it suitable for RF energy harvesting.

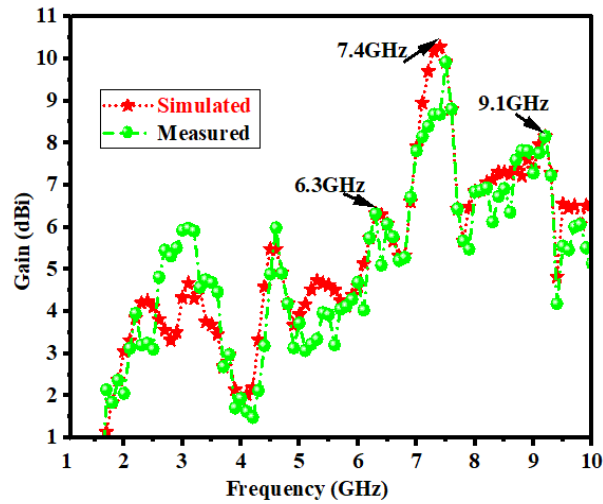


Figure 8. Simulated and measured gain at frequencies (a) 6.3 GHz and (b) 7.4 GHz and (c) 9.1 GHz.

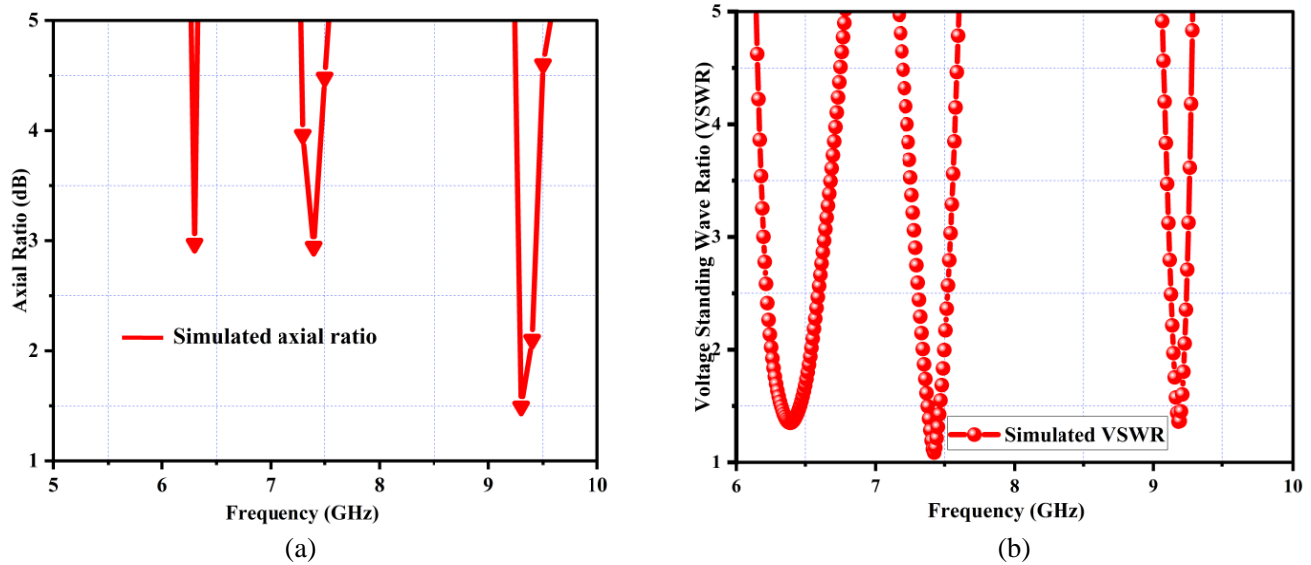


Figure 9. (a) Axial ratio and (b) VSWR at frequencies at 6.3 GHz, 7.4 GHz and 9.1 GHz.

4. DESIGN A RECTIFIER CIRCUIT FOR MULTIBAND CIRCULARLY POLARIZED ANTENNA

A rectifier circuit is simulated for the conversion of RF energy harvested using multiband microstrip patch antenna to DC power, as shown in Fig. 12. The rectifier receives input power from the antenna and converts it to DC output power. An impedance-matching network is used between the proposed antenna and the rectifier circuit for the highest power transfer. The efficiency of the proposed rectifier circuit can be calculated by using the equation [35].

$$\text{Efficiency \% } (\eta) = \frac{\text{Power DC}}{\text{Power RF}} \times 100 \tag{1}$$

$$\text{Power DC} = \frac{V^2 \text{ DC}}{RL} \tag{2}$$

Here, power DC = the power delivered to the load, Power RF = the rectifier’s input power.

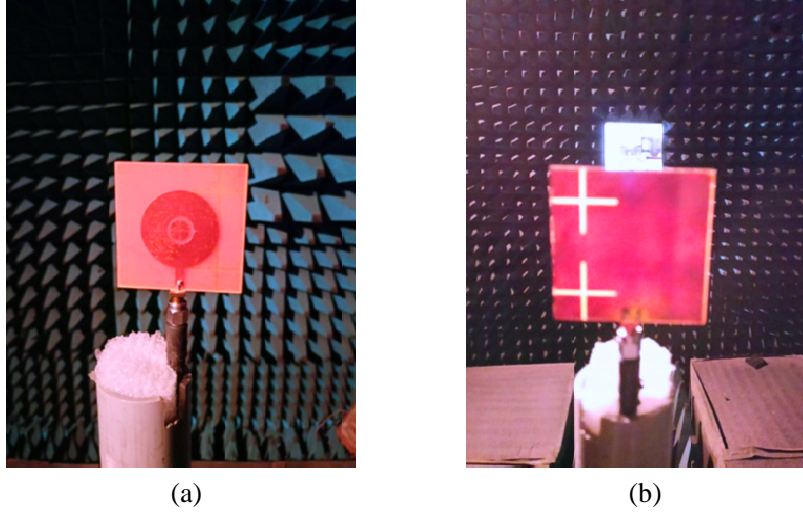


Figure 10. Testing in RF anechoic chamber, (a) front view and (b) back view.

Table 3. Antenna performance comparison with our research work.

References	Frequency (GHz)	Technique used	Overall Dimensions (mm)	Circularly polarized	Antenna gain (dB)
[29]	0.9, 1.8, 2.5 and 5.2	L-shaped Slots and DGS	48×42 ($\lambda_0/0.71$)	No	-
[38]	5.8	proximity-coupled feed	60×60 ($\lambda_0/0.86$)	Yes	6.0
[39]	2.4 and 5.8	CPW, Slot	50×40 ($\lambda_0/0.81$)	No	1.5, 4.2
[40]	0.9, 2, 5.5 and 7	Fractal, slots technique and CPW feed	60×60 ($\lambda_0/0.86$)	No	1, 3, 5, 4
This work	6.3, 7.4 and 9.1	Slots, slits and DGS	50×50 ($\lambda_0/0.80$)	Yes	6.32, 10.28 and 7.95

The load resistance of the rectifier at the output end is represented by RL [38]. The integration of the antenna structure with the rectifier forms a rectenna, which is used to provide continuous power to low-power sensors.

Table 4 shows the comparison of the proposed antenna to reference antennas in terms of size and conversion efficiency. The rectenna plays a significant function in an RF energy harvesting system because it harvests RF power and converts it to DC power.

5. MEASUREMENTS RESULTS OF THE FABRICATED ANTENNA AND RECTIFIER CIRCUIT

The fabricated prototype of the proposed antenna is depicted in Figs. 13(a) and (b). In Fig. 13(c), the simulated value of the reflection coefficient is compared to the measured outcome as evaluated in the Agilent Vector Network Analyzer (RF-VNA) model no. — KEYSIGHT P9372A which has frequency range 300 kHz–9 GHz for scattering parameters S_{11} . It is observed and shown in Fig. 14 that the simulated and measured outcomes seem comparable. Minor variations are caused by fabrication and measurement defects occurring during laboratory testing and can be neglected. The fabricated antenna has resonant frequency peaks at 6.3 GHz, 7.9 GHz, and 9.2 GHz, with a reflection coefficient

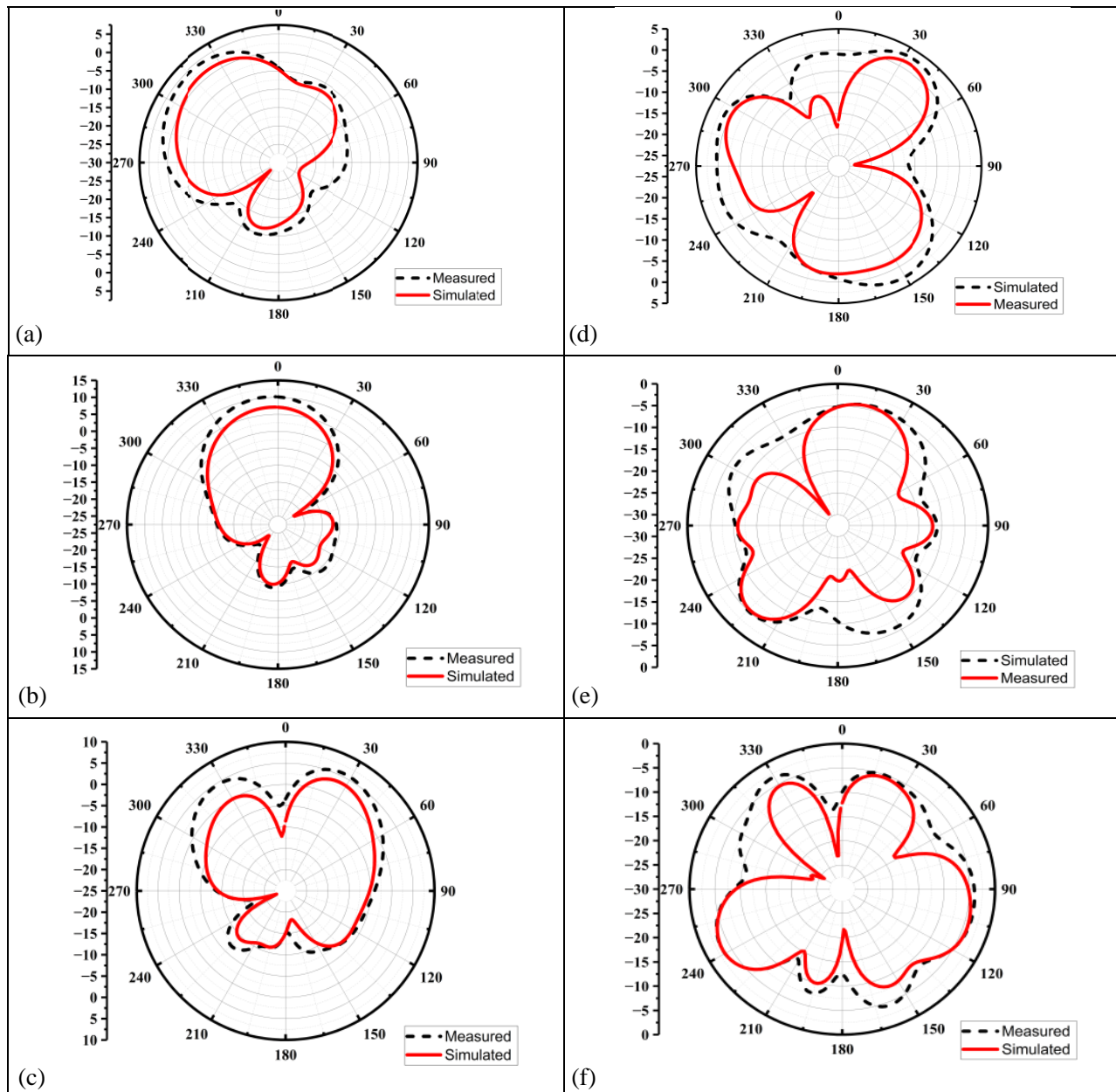


Figure 11. Simulated and measured radiation pattern plots in (a), (b), (c) *E*-plane and (d), (e), (f) *H*-plane at frequencies of 6.3 GHz, 7.4 GHz, and 9.1 GHz.

of -24.66 dB -37.3 dB and -32.50 dB, respectively. Figs. 15(a) and (b) show the comparison between simulated and measured VSWRs and axial ratios.

The complete test setup of fabricated RF energy harvesting receiver antenna and rectifier is shown in Figs. 16(a) and (b). The system rectifies voltage ranges from 5 mV to 64 mV which is suitable for low power sensors for charging the rechargeable battery.

Rectifier is simulated using electronic design software, and the received power obtained is 0.994 milliwatt with efficiency 25% at 6.3 GHz, 0.226 milliwatt with efficiency 56.76% at 7.4 GHz, and 0.129 milliwatt with efficiency 40.79% at 9.1 GHz. The received powers in all frequencies are sufficient to charge the battery required for operating low power sensors. The input power is varied from -20 dBm to 20 dBm and achieves 62 millivolt at an input power of -20 dBm. Fig. 17 depicts the simulated and

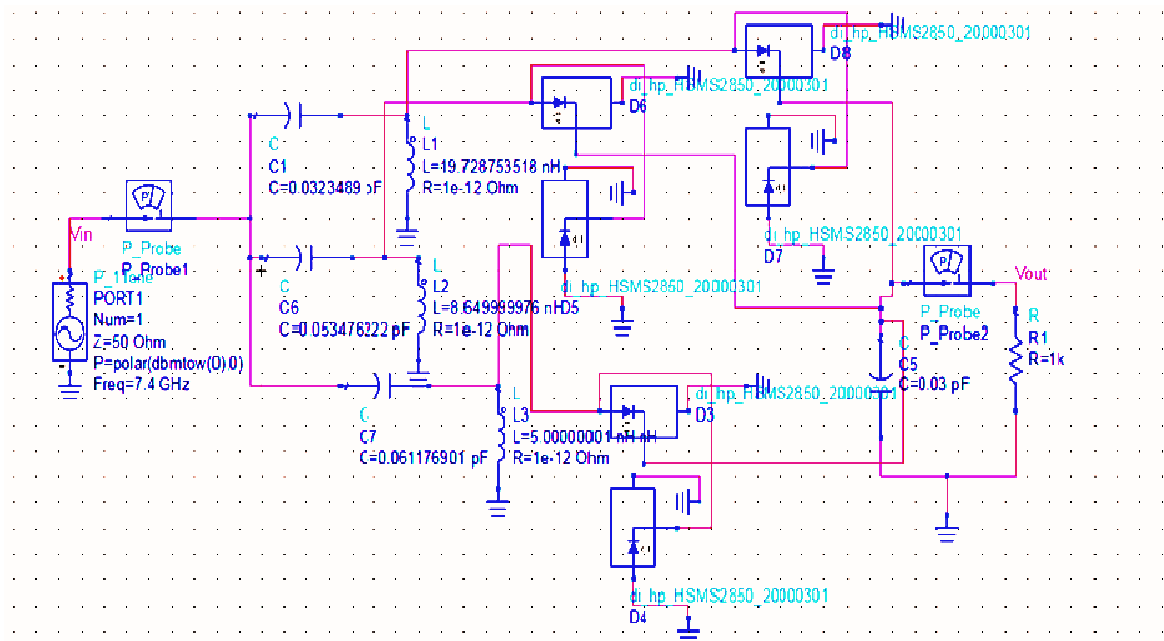


Figure 12. Combined voltage doubler simulation of a rectifier circuit for conversion of RF to DC power.

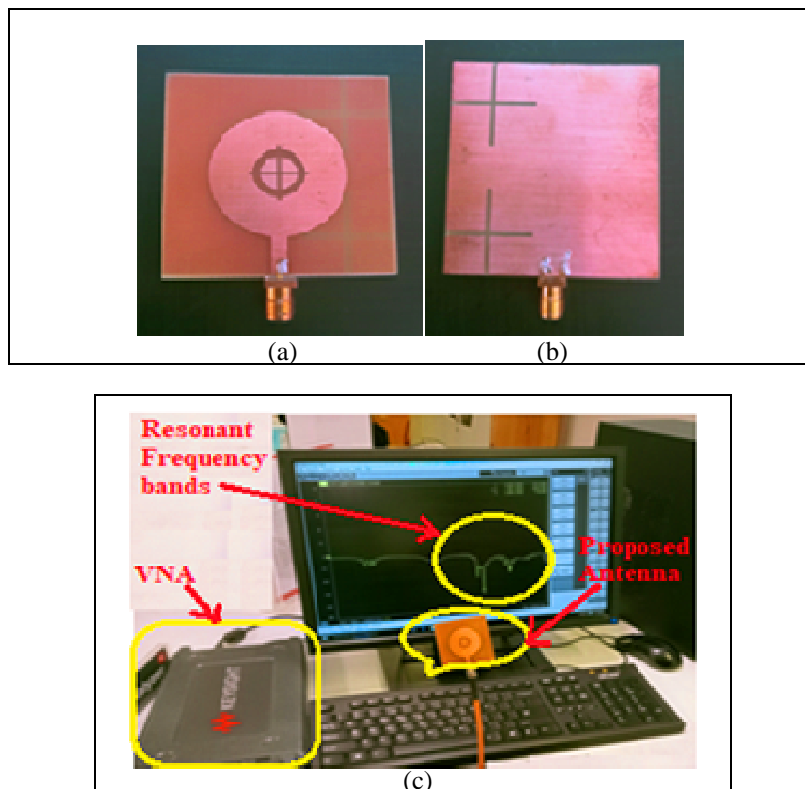


Figure 13. (a) Front view, (b) back view of fabricated antenna and (c) test setup of the proposed antenna using Vector Network Analyzer.

Table 4. The RF-DC conversion efficiency comparison between the other designed rectifier and the proposed rectifier.

References	Frequency (GHz)	Overall Dimensions (mm)	RF to DC Conversion Efficiency (%)
[32]	2.45	70 × 70	55%
[34]	1.8	45 × 45	61%
[37]	0.9 and 2.45	60 × 60	34%
[41]	0.83	80 × 80	44%
[42]	0.9 and 1.8	46 × 30	40.8%
[In this work]	6.3, 7.4 and 9.1	50 × 50	56.7%

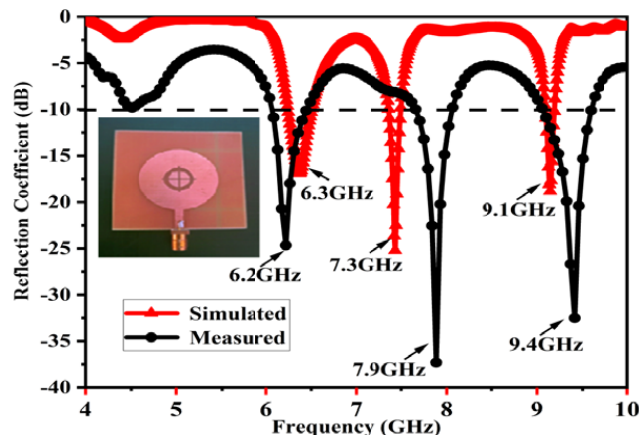


Figure 14. Comparison of the measured and simulated reflection coefficients.

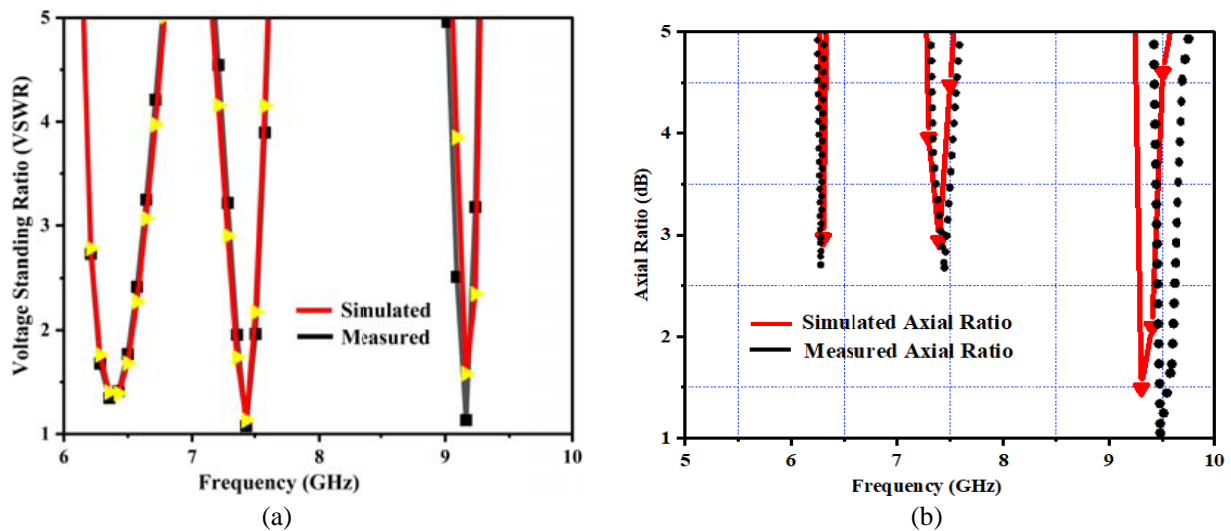


Figure 15. (a) Simulated and measured VSWR. (b) Simulated and measured Axial Ratio.

measured values of RF to DC conversion efficiency of the rectifier. Maximum value of simulated and measured RF to DC conversion efficiency is 56.76% and 51%, respectively. The simulated and measured results are in close approximation with each other.

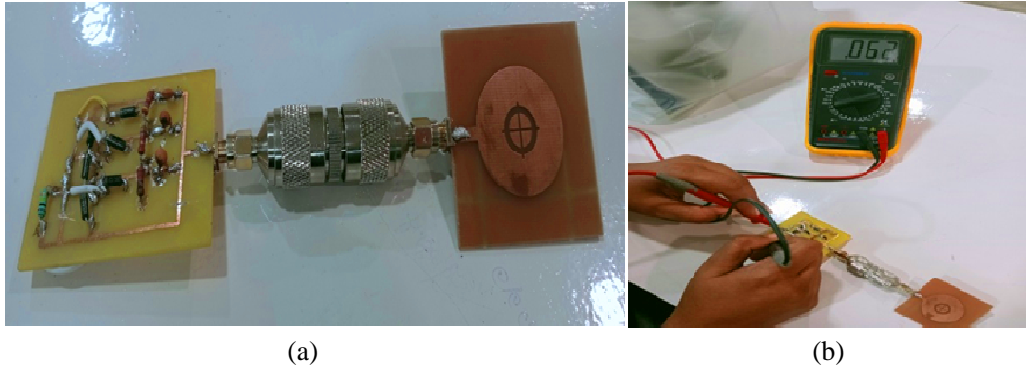


Figure 16. (a) Fabricated rectifier and (b) testing RF-DC output voltage for RF energy harvesting of proposed antenna system setup.

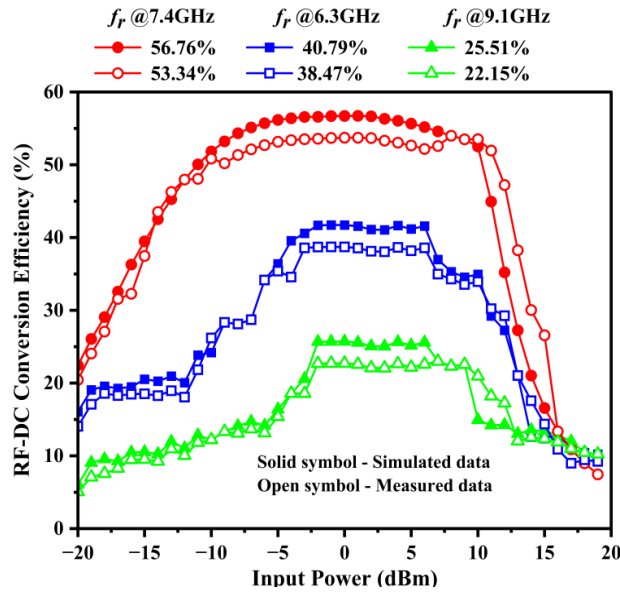


Figure 17. RF to DC conversion efficiency.

6. CONCLUSION

In this research paper, a multiband circularly polarized multiband microstrip antenna with a rectifier circuit is designed, simulated, and analyzed for energy harvesting. The designed antenna is circle-shaped with a dimensions 50×50 mm designed using a microstrip feed line, slits, annular slot, and DGS techniques. A step-by-step antenna evolution is performed, and optimized parameters are obtained to generate multiband band frequency response at frequencies 6.3 GHz, 7.4 GHz, and 9.1 GHz with obtained -10 dB bandwidths of 282 MHz, 178 MHz, and 81 MHz with circular polarization (axial ratio < 3 dB). The fabricated antenna has bandwidths of 195 MHz, 206 MHz, and 230 MHz, respectively with reflection coefficients of -24.66 dB, -37.3 dB, and -32.50 dB at resonant frequencies of 6.2 GHz, 7.8 GHz, and 9.3 GHz, respectively. The obtained measured gains are 6.3 dBi, 9.6 dBi, and 7.4 dBi at their respective frequencies. The RF energy harvested by the antenna is fed to the designed rectifier circuit for RF-DC conversion with achieved efficiency of 22% at 6.3 GHz, 53.34% at 7.4 GHz, and 38.47% at 9.1 GHz, respectively. Maximum measured efficiency of 53.34% is achieved at 7.4 GHz with -20 dBm input power at an associated load resistance of 1 k Ω . The proposed system is suitable for providing continuous power to low-power wireless sensor devices. Simulated and measured results are in good agreement and show that the proposed model is suitable for RF energy harvesting for low-power sensors applications.

REFERENCES

1. Muncuk, U., K. Alemdar, J. D. Sarode, and K. R. Chowdhury, "Multiband ambient RF energy harvesting circuit design for enabling batteryless sensors and IoT," *IEEE Internet of Things Journal*, Vol. 5, No. 4, 2700–2714, 2018.
2. Elkorany, A. S., A. N. Mousa, S. Ahmad, D. A. Saleeb, A. Ghaffar, M. Soruri, and E. Limiti, "Implementation of a miniaturized planar tri-band microstrip patch antenna for wireless sensors in mobile applications," *Sensors*, Vol. 22, No. 2, 667, 2022.
3. Azim, R., K. Dhar, M. S. Mia, and M. T. Islam, "Inset-fed microstrip patch antenna for ubiquitous wireless communication applications," *International Journal of Ultra Wideband Communications and Systems*, Vol. 5, No. 2, 57–64, 2022.
4. Khera, S., N. Turk, and N. Kaur, "Energy harvesting aspects of wireless sensor networks: A review," *Int. J. Recent Innov. Trends Comput. Commun.*, Vol. 5, No. 5, 875–878, 2017.
5. Aga, N., N. Agasimani, C. D. Bhushanagoudra, A. Pawar, and S. Naduvinamani, "Review on energy harvesting sources," *Indian Journal of Scientific Research*, 273–280, 2015.
6. Abdulhadi, A. E. and R. Abhari, "Multiport UHF RFID-tag antenna for enhanced energy harvesting of self-powered wireless sensors," *IEEE Transactions on Industrial Informatics*, Vol. 12, No. 2, 801–808, 2015.
7. Ibrahim, H. H., M. J. Singh, S. S. Al-Bawri, S. K. Ibrahim, M. T. Islam, A. Alzamil, and M. S. Islam, "Radio frequency energy harvesting technologies: A comprehensive review on designing, methodologies, and potential applications," *Sensors*, Vol. 22, No. 11, 4144, 2022.
8. Elsheakh, D., "Microwave antennas for energy harvesting applications," *Microwave Systems and Applications*, IntechOpen, 2017.
9. Ullah, M. A., R. Keshavarz, M. Abolhasan, J. Lipman, K. P. Esselle, and N. Shariati, "A review on antenna technologies for ambient RF energy harvesting and wireless power transfer: Designs, challenges and applications," *IEEE Access*, 2022.
10. Al-Yasir, Y. I., N. O. Parchin, M. N. Fares, A. Abdulkhaleq, M. Sajedin, I. T. Elfergani, J. Rodriguez, and R. Abd-Alhameed, "New high-gain differential-fed dual-polarized filtering microstrip antenna for 5G applications," *2020 14th European Conference on Antennas and Propagation (EuCAP)*, IEEE, 2020.
11. Divakaran, S. K. and D. D. Krishna, "RF energy harvesting systems: An overview and design issues," *International Journal of RF and Microwave Computer-Aided Engineering*, Vol. 29, No. 1, e21633, 2019.
12. Singh, D. and V. M. Srivastava, "Polarization insensitive 3D cylindrical shaped frequency selective surface," *2017 10th International Conference on Developments in eSystems Engineering (DeSE)*, IEEE, 2017.
13. Ramalingam, L., S. Mariappan, P. Parameswaran, J. Rajendran, R. S. Nitesh, N. Kumar, and B. S. Yarman, "The advancement of radio frequency energy harvesters (RFEHs) as a revolutionary approach for solving energy crisis in wireless communication devices: A review," *IEEE Access*, Vol. 9, 106107–106139, 2021.
14. Yusoff, S. S., S. A. Malik, and T. Ibrahim, "Simulation and performance analysis of a dual GSM band rectifier circuit for ambient RF energy harvesting," *Applications of Modelling and Simulation*, Vol. 5, 125–133, 2021.
15. Tang, X., G. Xie, and Y. Cui, "Self-sustainable long-range backscattering communication using RF energy harvesting," *IEEE Internet of Things Journal*, Vol. 8, No. 17, 13737–13749, 2021.
16. Sun, H. and W. Geyi, "A new rectenna using beamwidth-enhanced antenna array for RF power harvesting applications," *IEEE Antennas and Wireless Propagation Letters*, Vol. 16, 1451–1454, 2016.
17. Kashyap, N. and D. Singh, "Multiband slotted circular microstrip patch antenna with enhanced bandwidth for satellite applications," *2022 International Mobile and Embedded Technology Conference (MECON)*, IEEE, 2022.

18. Surender, D., M. A. Halimi, T. Khan, F. A. Talukdar, S. K. Koul, and Y. M. Antar, "2.45 GHz Wi-Fi band operated circularly polarized rectenna for RF energy harvesting in smart city applications," *Journal of Electromagnetic Waves and Applications*, Vol. 36, No. 3, 407–423, 2022.
19. Yadav, K., A. Chaturvedi, and G. K. Sharma, "Comparative study of antenna in RF-energy harvesting," *2022 2nd International Conference on Power Electronics & IoT Applications in Renewable Energy and Its Control (PARC)*, 1–7, IEEE, Jan. 2022.
20. Singh, M., D. Singh, G. Kumar, and R. Kumar, "A miniaturized and circularly polarized L-shaped slot antenna for ultra-wideband applications," *International Journal of Recent Technology and Engineering (IJRTE)*, Vol. 8, No. 4, ISSN: 2277-3878, Nov. 2019.
21. Singla, G. and R. Khanna, "Double-ring multiband microstrip patch antenna with parasitic strip structure for heterogeneous wireless communication systems," *International Journal of Microwave and Wireless Technologies*, Vol. 9, No. 8, 1757–1762, 2017.
22. Sah, B. K., G. Singla, and S. Sharma, "Design and development of enhanced bandwidth multi-frequency slotted antenna for 4G-LTE/WiMAX/WLAN and S/C/X-band applications," *International Journal of RF and Microwave Computer-Aided Engineering*, Vol. 30, No. 7, e22214, 2020.
23. Shen, S., C. Y. Chiu, and R. D. Murch, "A dual-port triple-band L-probe microstrip patch rectenna for ambient RF energy harvesting," *IEEE Antennas and Wireless Propagation Letters*, Vol. 16, 3071–3074, 2017.
24. Zahra, W. and T. Djerafi, "Ambient RF energy harvesting for dual-band frequencies below 6 GHz," *2018 IEEE Wireless Power Transfer Conference (WPTC)*, 1–2, IEEE, Jun. 2018.
25. Vu, H. S., N. Nguyen, N. Ha-Van, C. Seo, and M. T. Le, "Multiband ambient RF energy harvesting for autonomous IoT devices," *IEEE Microwave and Wireless Components Letters*, Vol. 30, No. 12, 1189–1192, 2020.
26. Kulkarni, J., R. K. Gangwar, and J. Anguera, "Broadband and compact circularly polarized MIMO antenna with concentric rings and oval slots for 5G application," *IEEE Access*, Vol. 10, 29925–29936, 2022.
27. Shen, S., Y. Zhang, C. Y. Chiu, and R. Murch, "An ambient RF energy harvesting system where the number of antenna ports is dependent on frequency," *IEEE Transactions on Microwave Theory and Techniques*, Vol. 67, No. 9, 3821–3832, 2019.
28. Kulkarni, J., C.-Y.-D. Sim, A. K. Poddar, U. L. Rohde, and A. G. Alharbi, "A compact circularly polarized rotated L-shaped antenna with J-shaped defected ground structure for WLAN and V2X applications," *Progress In Electromagnetics Research Letters*, Vol. 102, 135–143, 2022.
29. Agrawal, S., M. S. Parihar, and P. N. Kondekar, "A quad-band antenna for multi-band radio frequency energy harvesting circuit," *AEU-International Journal of Electronics and Communications*, Vol. 85, 99–107, 2018.
30. Pedram, K., J. Nourinia, C. Ghobadi, et al., "Compact and miniaturized metamaterial-based microstrip fractal antenna with reconfigurable qualification," *AEU-International Journal of Electronics and Communications*, Vol. 114, 152959, 2020.
31. Tran, H. H., N. Nguyen-Trong, and H. C. Park, "A compact dual circularly polarized antenna with wideband operation and high isolation," *Journal of RF and Microwave Computer Aided Engg.*, 1–9, Feb. 2020.
32. Ghosh, S., "Design and testing of RF energy harvesting module in GSM 900 band using circularly polarized antenna," *2015 IEEE International Conference on Research in Computational Intelligence and Communication Networks (ICRCICN)*, IEEE, 2015.
33. Garlapati, P., H. Chilaka, M. Rangu, R. Chigula, and S. Chilukuri, "A circularly polarized multiband multimode SIW antenna," *2020 11th International Conference on Computing, Communication and Networking Technologies (ICCCNT)*, 2020.
34. Mouapi, A., N. Hakem, and N. Kandil, "High efficiency rectifier for RF energy harvesting in the GSM band," *2017 IEEE International Symposium on Antennas and Propagation & USNC/URSI National Radio Science Meeting*, IEEE, 2017.

35. Ali, W., H. Subbyal, L. Sun, and S. Shamoon “Wireless energy harvesting using rectenna integrated with voltage multiplier circuit at 2.4 GHz operating frequency,” *Journal of Power and Energy Engineering*, Vol. 10, No. 3, 22–34, 2022.
36. Elsheakh, D., M. Farouk, H. Elsadek, and H. Ghali, “Quad-band rectenna for RF energy harvesting system,” *Journal of Electromagnetic Analysis and Applications*, Vol. 12, No. 5, 57–70, 2020.
37. Singh, N., B. K. Kanaujia, M. T. Beg, et al., “Low profile multiband rectenna for efficient energy harvesting at microwave frequencies,” *International Journal of Electronics*, Vol. 106, No. 12, 2057–2071, 2019.
38. Sun, H. and W. Geyi, “A new rectenna using beamwidth-enhanced antenna array for RF power harvesting applications,” *IEEE Antennas and Wireless Propagation Letters*, Vol. 16, 1451–1454, 2017, doi: 10.1109/LAWP.2016.2642124.
39. Wong, K.-L., H. J. Chang, C. Y. Wang, and S. Y. Wang, “Very-low-profile grounded coplanar waveguide-fed dual-band WLAN slot antenna for on-body antenna application,” *IEEE Antennas and Wireless Propagation Letters*, Vol. 19, No. 1, 213–217, 2019.
40. Singh, N., B. K. Kanaujia, M. T. Beg, Mainuddin, S. Kumar, H. C. Choi, and K. W. Kim, “Low profile multiband rectenna for efficient energy harvesting at microwave frequencies,” *International Journal of Electronics*, Vol. 106, No. 12, 2057–2071, Dec. 2019.
41. Kanaya, H., S. Tsukamaoto, T. Hirabaru, D. Kanemoto, R. K. Pokharel, and K. Yoshida, “Energy harvesting circuit on a one-sided directional flexible antenna,” *IEEE Microwave and Wireless Components Letters*, Vol. 23, No. 3, 164–166, 2013.
42. Ho, D.-K., I. Kharrat, V. D. Ngo, T. P. Vuong, Q. C. Nguyen, and M. T. Le, “Dual-band rectenna for ambient RF energy harvesting at GSM 900 MHz and 1800 MHz,” *2016 IEEE International Conference on Sustainable Energy Technologies (ICSET)*, IEEE, 2016.